EINDHOVEN UNIVERSITY OF TECHNOLOGY

Eindhoven University of Technology

BACHELOR

1/f noise in ferromagnetic tunnel junctions

Grundmann, J.

Award date:
2000

Link to publication

Disclaimer
This document contains a student thesis (bachelor's or master's), as authored by a student at Eindhoven University of Technology. Student theses are made available in the TU/e repository upon obtaining the required degree. The grade received is not published on the document as presented in the repository. The required complexity or quality of research of student theses may vary by program, and the required minimum study period may vary in duration.

General rights
Copyright and moral rights for the publications made accessible in the public portal are retained by the authors and/or other copyright owners and it is a condition of accessing publications that users recognise and abide by the legal requirements associated with these rights.

- Users may download and print one copy of any publication from the public portal for the purpose of private study or research.
- You may not further distribute the material or use it for any profit-making activity or commercial gain

Take down policy
If you believe that this document breaches copyright please contact us providing details, and we will remove access to the work immediately and investigate your claim.

Download date: 15. May. 2025

Eindhoven University of Technology
Department of Physics
Group Physics of Nanostructures

1/f Noise in Ferromagnetic Tunnel Junctions

Jens Grundmann

March 2000

Report of a traineeship under the supervision of Ir. A.A. Smits.

Abstract

In this project 1/f noise in a ferromagnetic tunnel junction was observed. Both the field and current dependence was measured. The results show, that the 1/f noise depends on the alignment of the magnetisations of the two ferromagnetic layers. In the antiparallel case the noise level is higher than in the parallel one. If the magnetisation of one ferromagnet switches a peak in the 1/f noise appears.
High currents lower the noise level in the antiparallel state while it stays constant in the parallel state. For high currents the magnetisation of the biased layer switches at lower fields, therefore the antiparallel state becomes smaller. This is caused by a warming up of the sample.
Because of the two different 1/f noise levels a noise ratio similar to the MR-ratio is defined and compared with calculations with the Julliere model and a free electron model.

Contents

I Theory 3

1 Magnetoresistance Effects 4
1.1 Ordinary Magnetoresistance Effect 4
1.2 Anisotropic Magnetoresistance Effect 6
1.3 Giant Magnetoresistance Effect 6
1.4 Tunnel Magnetoresistance Effect 7

2 Tunneljunction 9
2.1 Tunnel Current 9
2.2 Tunnel MR-Ratio 10

3 Noise 13
3.1 Mathematical Background 13
3.1.1 Random Pulse Train 13
3.1.2 Spectral Noise Intensity 13
3.2 Shot Noise 14
3.3 Thermal (Johnson) Noise 14
3.4 White Noise in Tunnel Junctions 15
3.5 1/f Noise 16

II Experiment 17

4 Experimental Setup 18
4.1 Samples 18
4.2 Experiment 18

5 Measurements 22
5.1 Resistance versus Field 22
5.2 Current dependence of the MR-Ratio 22
5.3 White Noise 24
5.4 $1/f$-Noise 24
5.4.1 $1/f$-Noise versus Field 24
5.4.2 Current dependence of $1/f$-Noise 24

6 Discussions 27

Introduction

During a traineeship on the TU Eindhoven for four month I observed noise in ferromagnetic tunnel junctions. Primarily the $1/f$-noise and its dependence of both field H and current I was investigated. The following report should give an overview about the things behind it and the things I've done.
The first part includes some considerations about the theory such as magneto resistance effects, tunnel current, noise theory and different types of noise. In the section about the magneto resistance effects mainly in the GMR and TMR-effect are considered. The OMR and AMR are described only in a short way, especially for the last one I have to advert to the corresponding articles, mainly because it is very difficult to understand and to explain. The section about the different kinds of noise describes only those that can be found in ferromagnetic tunnel junctions.
The second part reports the results of my measurements. First something about the magnetoresistance ratio and its dependence on the applied field and the current is writen. The main parts of the measurements was the 1/f noise. It depends strongly on the field, especially on the alignment of the magnetisation direction of the two ferromagnets. Also a dependence on the current is measured. At the end of this chapter I compare the measurements with two theoretical model, the Julliere and the free electron model.

Part I

Theory

Chapter 1

Magnetoresistance Effects

The following section describes the known magnetoresistance effects in a very short way to point out the differences between these effects. All are caused by a change of the magnetic structure on a nanometer scale. The first two effects, the *ordinary magnetoresistance effect (OMR)* and the *anisotropic magnetoresistance effect (AMR)* are known for a long time, but the third one, the *giant magnetoresistance effect (GMR)* discovered in 1988 and the last one, the *tunnel magnetoresistance effect (TMR)* found in 1995, are relatively new.

1.1 Ordinary Magnetoresistance Effect

The ordinary MR effect is caused by the Lorentz force and occured in both conductors and semiconductors. When electrons are moving through the material with the speed $\vec{v}$ caused by a potential U and there is an induction $\vec{B}$, then the electron experiences a force, called the Lorentz force $\vec{F}$,

$$\vec{F} = -e(\vec{v} \times \vec{B}). \tag{1.1}$$

This force causes that the trajectory of the electron is not a line anymore, but a curve (figure 1.1). This causes a longer way for the electrons, which means a higher resistance in a homogeneous material. Because the resistance depends on a magenetic field, it is called magnetoresistance (MR) effect.
It is not a strong effect, because for a high field of e.g. $\vec{B} = 1\text{T}$ the ordinary MR effect is less than 1%. As an important difference with other MR effects this effect does not not depend on the magnetisation of the material but only on the magnetic induction and the speed of the electrons. Because of the low effect and high fields there is no practical use for this type of sensor.
Similar to ordinary MR effect is the Hall effect. The experimental construction is the same as for the OMR: a strip of a material finite in the x-direction, a current in the $-$y-direction and an induction through the material in z-direction. The Lorentz force on the electrons is in this case antiparallel to the x-axis. Due to this force the number of electrons on both sides of the material is different leading to an electric field, and therefore a force parallel to the x-direction (Figure 1.2). The direction of this force is antiparallel to the Lorentz forces F_L and in the equilibrium the resulting force on the electrons in x-direction is zero. In this case the trajectorie of the electrons becomes straight again.
The voltage caused by the electrical field is called Hall voltage U_H. In the first approximation the Hall voltage is a linear function of the Induction $\vec{B}$. This is why the main application of the Hall effect are field sensor.

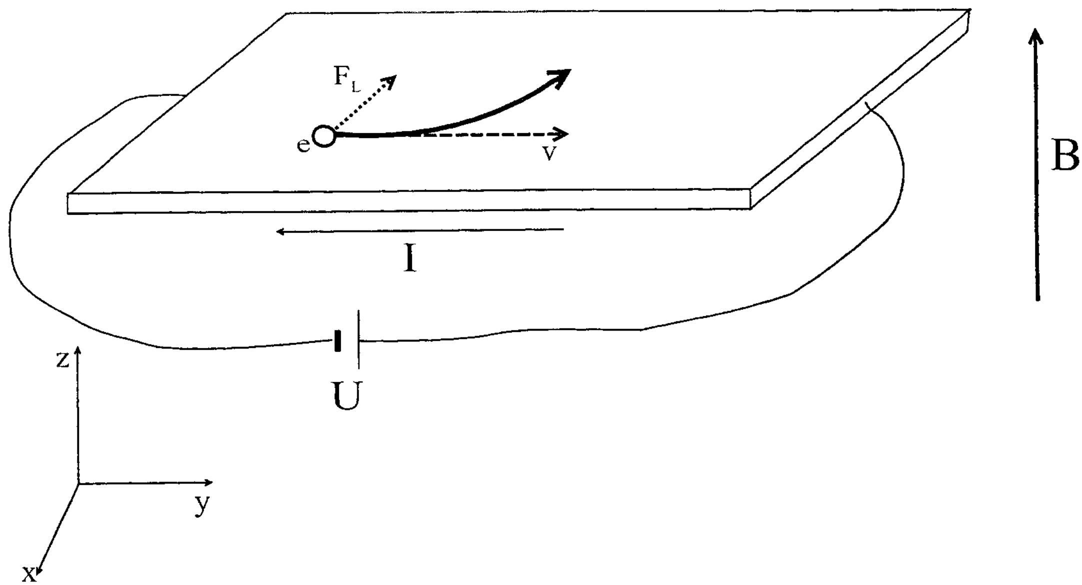

Figure 1.1: When an electron moves through a sample with a magnetic induction B the trajectorie changes due to the Lorentz force F_L.

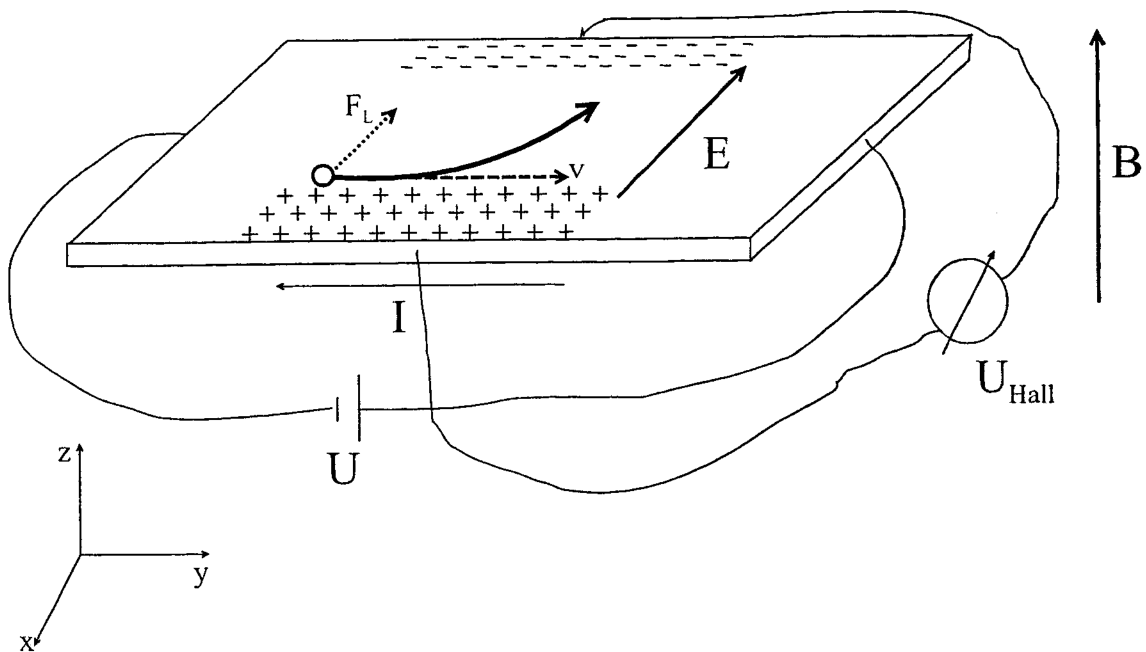

Figure 1.2: Due to the Lorentz force F_L more electrons are on one side of the material than on the other. The resulting voltage is the Hall voltage U_{Hall}.

1.2 Anisotropic Magnetoresistance Effect

William Thomson discovered, that the resistance of a ferromagnet depends on the magnetisation and the direction of the current, in 1857. The origin is a relativistic effect, which could not be explained until the 1950s [1]. It is observed in different ferromagnetic materials such as Fe, Co or Ni. As already mentioned the resistance of the material depends on the angle between the magnetisation M and the current I. If the current is perpendicular to the magnetisation, the resistance $\rho_\perp$ is lower than the resistance $\rho_\parallel$ in the case with a current parallel to the magnetisation. The AMR-ratio is defined as

$$\frac{\Delta\rho}{\rho_{AV}} = \frac{\rho_\parallel - \rho_\perp}{\frac{1}{3}\rho_\parallel + \frac{2}{3}\rho_\perp}, \tag{1.2}$$

where $\rho_{AV} = \frac{1}{3}\rho_\parallel + \frac{2}{3}\rho_\perp$.
MR ratio's of 25% at 4.2K or 6.5% at 290K are possible, that means that this effect is bigger than the ordinary MR effect. Because of the higher ratio, there are more applications for the AMR such like magnetic field sensors or read heads for magnetic disk andtape recording.
The origin of the AMR is the anisotropy of a ferromagnetic material: the resistance perpendicular to the magnetisation is lower than parallel to it. It can be explained using the band structure for metals. All materials in which the AMR is observed have a 3d-band and a s-band at the Fermi level. Both bands are very close together, therefore the electrons have a high probability to scatter from the s-band into the d-band [1].
The s-electrons contribute more to the current than the d-electrons, because they have a higher mobility. But the resistance of the s-electrons is due to scattering into the d-bands and because these bands are not spherical like the s-bands the resistance changes depending on the angle between the current and the magnetisation.

1.3 Giant Magnetoresistance Effect

The Giant magnetoresistance effect is a very important effect, because in general the MR ratio is much larger than in all previous effects. It took a long time after the AMR till the GMR was discovered. In 1988 Grünberg [2] saw and described the GMR for Fe/Cr/Fe element (figure 1.3) deposited on a flat substrate. Cr is an antiferromagnetic

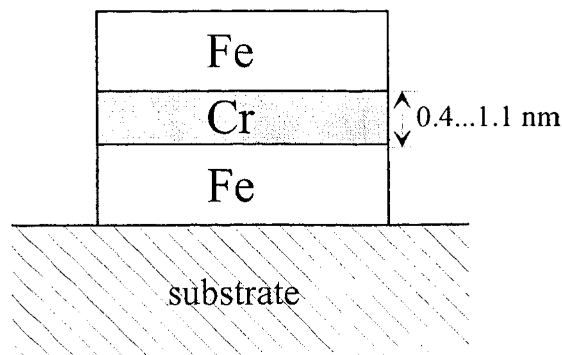

Figure 1.3: This is the schematic structure of the GMR element Grünberg used in 1988, two Fe layers seperated by a Cr layer with a thickness changing from 0.4 nm to 1.1 nm.

(AF) and Fe a ferromagnetic metal (FM). Both magnetisations of the Fe layers are coupled

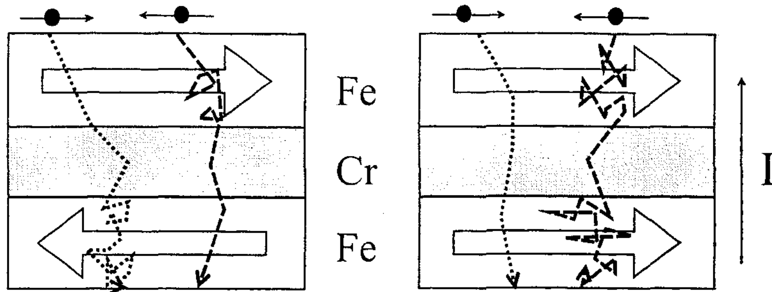

Figure 1.4: Both pictures show the movement of an electron through a GMR element; the left one for antiparallel and the right one for parallel alignment of the magnetisation directions of the layers. Electrons with a spin parallel to the magnetisation have a low resistance and antiparallel aligned spins make a high resistance.

antiferromagnetical, if the Cr layer is thin enough (around 0.8nm). Antiferromagnetic coupling means that the magnetisations want to stay in the antiparallel at zero field. There is a certain field necessary to overcome this coupling and to move both magnetisations in the same direction as the magnetic field. This position is called parallel position. The new thing Grünberg saw is, that this change of the orientation of the magnetisation direction of the layers causes a change in the resistance. For very low temperatures very high MR ratio's are possible e.g. for Fe/Cr multilayers 90% at $4.2K$ or 220% at $1.5K$ are measured, but also for room temperature several tens of percent are measured. Because of these high values compared to the known MR-effects this effect was called giant magnetoresistance effect.
This effect can be explained by a spin dependent scattering probability and the magnetic layer acting as a spin filter: only the electrons with a spin parallel to the magnetisation direction can pass and for the electrons with the other spin directions the resistance of the layer is very high (figure 1.4). When both magnetisations are parallel aligned the resistance for one spin channel (spin direction parallel to the magnetisation) is low, for the other one (spin direction antiparallel to the magnetisation) very high and the total resistance is low. But when the magnetisations are antiparallel the resistance of both spin channels is high, because for each spin channel there is one layer, in which the electrons are scattered. That means, the total resistance in this case is higher than in the parallel case.

1.4 Tunnel Magnetoresistance Effect

The TMR effect was discovered already in 1975 [3], but only after 1995 [4] it was possible to produce tunnel junctions with a high MR-ratio at room temperature. Such a tunnel junction consist of two magnetic layers seperated by a nonmagnetic insulating layer (figure 1.5).
In classical physics it would not be possible to drive a current through this structure because of the insulating layer. But in the quantum physics there is a small probability for an electron to tunnel through this barrier if this barrier is thin enough.
If the conducting layers are made of a ferromagnetic material than the magnitude of the tunnel current depends on the angle between the magnetisation directions of the two layers. The reason for this effect is the dependence of the tunnel probability of an electron through a barrier on its spin direction, see chapter 2.

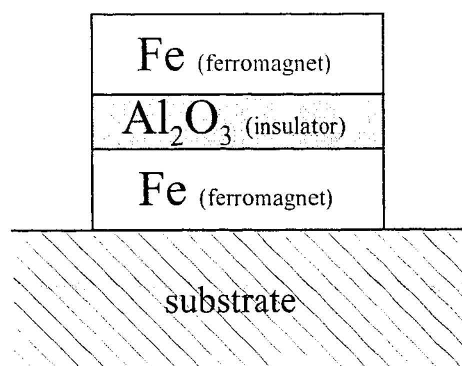

Figure 1.5: The structure of a TMR element consist of two ferromagnets (in this case Fe) seperated by an insulating oxide layer (here Al_2O_3).

Chapter 2

Tunneljunction

2.1 Tunnel Current

To derivate an expression for the tunnel current the free electron model [5] can be used, which is based on the following two assumptions. First, there is no interaction between the electrons and second, the electron is a free particle inside the crystal. With this model the electrons in the electrodes are described.
The tunnel process itself is a quantum mechanical phenomena and to calculate the tunnel current it is necessary to solve the Schrödinger equation

$$-\frac{\hbar^2}{2m}\Delta\varphi(\vec{r}) + U(\vec{r})\varphi(\vec{r}) = E\varphi(\vec{r}),^1 \tag{2.1}$$

where φ is the wave function of the electron.
The two electrodes are infinite thick and their potential is assumed to be constant (figure 2.1). Between them is a rectangular barrier with the thickness d. The potential U of it is higher than the energie E of the electrons in the electrodes, which can have a energy between 0 and the Fermi level E_{FL}. When a voltage is applied to the junction, the barrier becomes trapeziform.
Using this the wave function φ can be calculated. By dividing the amplitudes of φ on the left and the right side (figure 2.1) the probability for an electron to cross the barrier can be obtained. For a rectangular barrier this probability, called Transmission $T(E)$, is

$$T(E) = \frac{16E(U-E)}{U^2}e^{-(2d/\hbar)\cdot\sqrt{2m(U-E)}}. \tag{2.2}$$

Now the tunnel current I can be calculated by using the following integral

$$I = \int_{-\infty}^{\infty} N(E)T(E)\,dE. \tag{2.3}$$

$N(E)$ is the so called supply function, which contains the dependence of the number of participating electrones on the applied voltage V_B and the temperature,

$$N(E) = \frac{mk_BeT}{2\pi^2\hbar^3}\ln\left(\frac{1+\exp\left(\frac{E_{FL}-E}{k_BT}\right)}{1+\exp\left(\frac{E_{FL}-eV_B-E}{k_BT}\right)}\right). \tag{2.4}$$

[1] This is time independent Schrödinger equation. Note that for an exact description the more difficult time dependend Schrödinger equation has to be solved! [Lit]

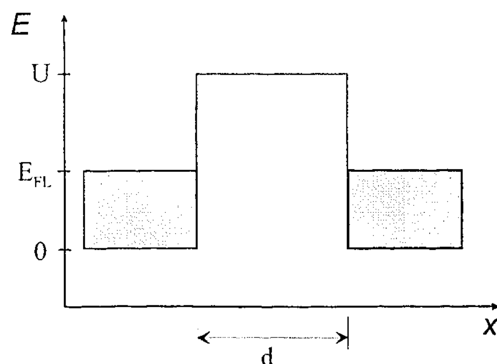

Figure 2.1: The schematic model for the potential of two conductors seperated by a barrier with a thickness d. U is the potential of the barrier and E_{FL} the Fermi level of the conductors.

Because of the exchange splitting the energies are different for the spin up $\uparrow$ and spin down $\downarrow$ electrons. Also the energy level differ for the parallel and antiparallel alignement of the magnetisations [5]. Therefore different currents exist for both the two alignments (I_P and I_{AP}) and the two spin channels ($I_P^{\uparrow}$ and $I_P^{\downarrow}$ respectively $I_{AP}^{\uparrow}$ and $I_{AP}^{\downarrow}$),

$$I_P = I_P^{\uparrow} + I_P^{\downarrow} \quad (2.5)$$

$$I_{AP} = I_{AP}^{\uparrow} + I_{AP}^{\downarrow}. \quad (2.6)$$

Using this the MR-ratio can be get:

$$MR = \frac{I_P - I_{AP}}{I_{AP}} \quad (2.7)$$

2.2 Tunnel MR-Ratio

The following calculations to understand the TMR effect are based on the Julliere model [3]. He made the assumption, that the tunnel current is for both the parallel and the antiparallel state I_P and I_{AP} is proportional to the product of the effective tunneling density of states, which means in principle the density of states at the Fermi-level. For every spin channel

$$I \sim N_1 N_2. \quad (2.8)$$

This leads to (see figure 2.2)

$$I_P = N_1^{\uparrow} N_2^{\uparrow} + N_1^{\downarrow} N_2^{\downarrow}, \quad (2.9)$$

$$I_{AP} = N_1^{\uparrow} N_2^{\downarrow} + N_1^{\downarrow} N_2^{\uparrow}, \quad (2.10)$$

where N_1 are the densities of states for the a channel of the first ferromagnet and N_2 are the same for the second ferromagnet.
The MR-ratio is

$$MR = \frac{I_P - I_{AP}}{I_P} = \frac{2P_1P_2}{1 + P_1P_2}, \quad (2.11)$$

with the polarisation P

$$P = \frac{N^{\uparrow} - N^{\downarrow}}{N^{\uparrow} + N^{\downarrow}}. \quad (2.12)$$

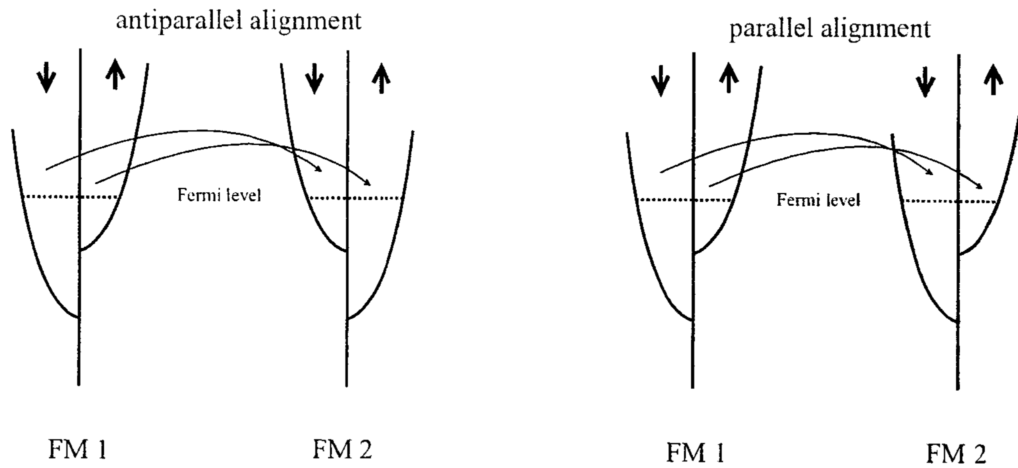

Figure 2.2: The left figure shows the tunneling of the electrons for the antiparallel and the right one for the parallel state. The Julliere model assume, that the spin direction is conserved during tunneling. $I_P = I_P^{\uparrow} + I_P^{\downarrow}$ and $I_{AP} = I_{AP}^{\uparrow} + I_{AP}^{\downarrow}$.

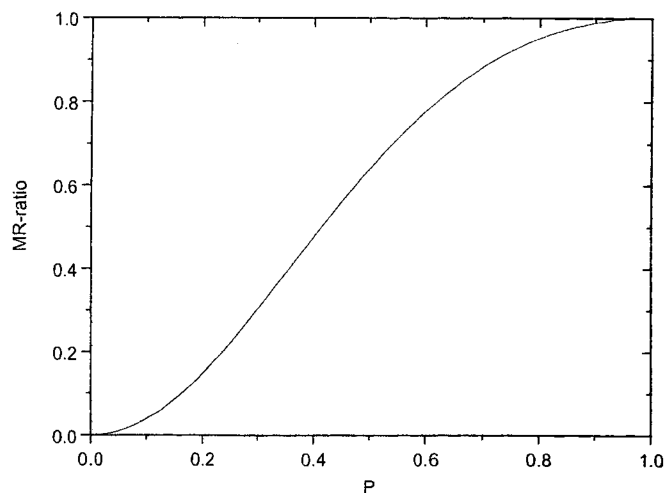

Figure 2.3: This is the MR-ratio depending on the polarisation $P = P_1 = P_2$ predicted by the Julliere model.

If the polarisation is known, it is easy to calculate the MR-ratio. How ever it is not possible to measure the polarisation in an exact way but only using indirect methods, which lead often to different results. Also the calculated MR-ratio is not consistent with the one out of theoretical calculation.
An interesting prediction of this model is the independence of the MR-ratio on both the geometrie and the electronic structure of the barrier, which seemed to be not alright, because as shown above the tunnel probability of an electron depends on the structure of the barrier, so one would expect, that this is also true for the MR-ratio.
In the model of Slonczewski [6] this is taken into account.

Chapter 3

Noise

3.1 Mathematical Background

3.1.1 Random Pulse Train

Noise in electronic devices is a small randomly varying function of time on your signal. The fluctuations are neither reproducible nor predictable, but some statistical properties, like the variance of the signal, can be obtained by making many observations of the process.
The origin of noise is often a large number N of independent events. The superposition of the event shapes $f(t)$ gives the noise waveform $x(t)$,

$$x(t) = \sum_{i=1}^{N} a_i f(t - t_i), \tag{3.1}$$

a_i is the amplitude of the ith event and t_i is the time at which it occurs. This is called random pulse train.

3.1.2 Spectral Noise Intensity

The noise can be studied in the time domain, but more information can be obtained, when the signal is transformed to the frequency domain. This is done by using the Fourier transformation and the result is the Fourier transformed $X_T(\omega)$ of the signal $x(t)$. Using this the spectral noise intensity $\overline{S_x(\omega)}$ can be derivated,

$$\overline{S_x(\omega)} = \lim_{T\to\infty} \frac{2\overline{|X_T(\omega)|^2}}{T} \tag{3.2}$$

where T means the duration of the measurement and the bar denotes an average either over the time or the ensemble. For a time average the noise is measured for a long time and then the average value of $x(t)$ can be calculated as

$$\overline{x} = \lim_{T\to\infty} \frac{1}{T} \int_{-\frac{T}{2}}^{\frac{T}{2}} x(t)\, dt. \tag{3.3}$$

To get the ensemble average the noise is measured on a N[1] identical systems. The way of measuring and the structure has to be the same for all of them. In this case the average

[1] with $N > 1$

of $x(t)$ is

$$\overline{x(t)} = \lim_{N\to\infty} \frac{1}{N} \sum_{i=1}^{N} x_i(t), \tag{3.4}$$

where $x_i(t)$ is the random value of the i-th system at the time t. An interesting question is now, if both lead to the same result. Processes in which this is true are called *ergodic*, otherwise it is *nonergodic*.
In genereal a time average is done and one assumes, that the system is ergodic.

3.2 Shot Noise

The origin of shot noise is the discrete nature of an electron. Each electron gives a pulse in the current. The average current is the sum over all the N electrons with the charge e crossing the barrier in a certain time t:

$$I = -\frac{N \cdot q}{t}. \tag{3.5}$$

The minus is caused by the difference between the current direction and the direction of the movement of the electrons.
According to (3.5) the current is the sum over all tunneling electrons. Because the time duration of the tunneling process is infinitesimal, the δ-function can be used instead of f and (3.5) becomes

$$i(t) = -q \sum_{k=1}^{N} \delta(t - t_k), \tag{3.6}$$

where t_k is the moment, the k-th electron tunnels. The t_k have the values, that the number of electrons are Poisson distributed [7]. Using this equation, the current noise spectrum S_I can be calculated [8, 9]),

$$S_I(\omega) = 2qI. \tag{3.7}$$

This means, that the shot noise does not depend on the frequency (white), but only on the current.

3.3 Thermal (Johnson) Noise

Thermal noise was observed first by Johnson in 1927/28 on a resistor in thermal equilibrium. It is caused by the electrons moving randomly through the material due to their thermal energie.
The power spectrum can be calculated by using the assumption that fluctuations are a result of a large number of independent, random events. An event is here an initial action, caused for example by collision with other electrons, which pulls the electron out of its equilibrium state. After that the electron moves back again to its original position. This movement results in a change in the voltage or current. The result is a noise spectrum, which does not depend on U or I and it can even be measured at $U = 0$. It is also independent of the frequency. It depends on both temperatur T and resistance R [8, 9]:

$$S_I(\omega) = \frac{4kT}{R} \tag{3.8}$$

$$S_V(\omega) = 4kTR \tag{3.9}$$

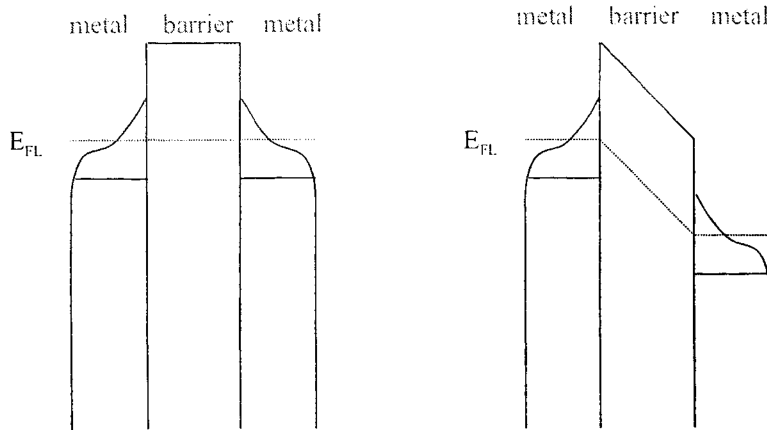

Figure 3.1: The left picture shows the two metals separated by an insulator in the case of no applied voltage. The number of electrons for tunneling (grey part) on both sides is the same, so the resulting current I is zero. The right picture shows the same with an applied voltage U. Now there are no electrons on the right available for the tunnel process and the resulting current $I > 0$ is from the right to the left.

Note, that in general it is possible to measure the noise of the voltage or the noise of the current. Each results a different spectral noise intensity, $\overline{S_V(\omega)}$ and $\overline{S_I(\omega)}$. With the following equation it is possible to convert them:

$$\overline{S_I(\omega)} = \overline{S_V(\omega)} \left(\frac{dI}{dV}\right)^2 \Bigg|_{I,V} . \tag{3.10}$$

3.4 White Noise in Tunnel Junctions

Untill now two kinds of white noise are described, the Johnson noise and the thermal noise. In this section the white noise level in a tunnel junction is deriveded [10, 9].
The white noise in a tunnel junction is caused by shot noise. Electrons can only tunnel from an occupied state to an unoccupied state. When there is no voltage over the junction, on both sides are occupied and unoccupied states available for the tunnel process. Therefore two tunnel currents are present $I_{r\to l}$ and $I_{l\to r}$[2]. The resulting current I to the right is then,

$$I = I_{r\to l} - I_{l\to r}. \tag{3.11}$$

In this case the tunnelcurrent from the left to the right is the same as for the right to the left, I is zero in this case.
When a voltage U is applied over the tunnel junction, the energy E of the electrons on the right electrode becomes lower. Then there are less unoccupied states on the left available for the electrons on the right to tunnel to. In this case $I_{r\to l}$ becomes higher than $I_{l\to r}$ and a net current I can be measured.
The relation between $I_{l\to r}$ and $I_{r\to l}$ is [10],

$$I_{r\to l} = I_{l\to r} e^{\frac{qV}{kT}}. \tag{3.12}$$

[2]Note, that the direction of the current I is antiparallel to the direction of the moving electrons!

Both currents produce shot noise and if $I_{l\to r}$ and $I_{r\to l}$ are uncorrelated, their noise power can be added. Using (3.7) the current noise power becomes

$$S_I = 2q(I_{l\to r} + I_{r\to l}). \tag{3.13}$$

Together with (3.11) and (3.12) the spectral noise power $S_I(\omega)$ is

$$S_I(\omega) = 2qI\coth(\frac{qV}{2kT}). \tag{3.14}$$

There are two limiting cases, $qV > 2kT$ and $qV < 2kT$. In the first case the equation becomes

$$S_I(\omega) = 2qI, \tag{3.15}$$

and in the second one

$$S_I(\omega) = \frac{4kT}{R} \qquad \text{with} \qquad R = lim_{I\to 0}\frac{V}{I}. \tag{3.16}$$

That means the Johnson noise and the shot noise are special cases of (3.14).

3.5 1/f Noise

It is only seen at low frequencies and decreases with nearly $1/f$. The origin of this kind of noise is unknown, but there are some models, which describe it more or less well. A empirical model is the Hooge relation [11] for homogeneous samples:

$$S_V(f,H) = \frac{\alpha(H)V^2}{Nf^\gamma} \tag{3.17}$$

where N is the number of charged particles, γ a constant close to 1 and $\alpha(H)$ the Hooge constant which has found to be a constant for homogeneous samples with a value of 2×10^{-3}.

Recently 1/f noise of magnetoresistive elements have been measured. There they found, that the 1/f noise intensity depends on the applied magnetic field. The explanation for this field dependence was, that the magnetisation fluctuates, which in turn produces fluctuations in the resistance. This means, that where the sensor is the most sensitive, the noise is much higher [12].

Part II

Experiment

Chapter 4

Experimental Setup

4.1 Samples

The samples are deposited at Philips by sputtering and consist of nine layers, see figure (4.1). On top is a Ta layer to protect the junction from oxidation. The tunnel junction itself consists of two ferromagnets seperated by a insulator. The ferromagnets are build of a $Ni_{80}Fe_{20}$ (Py) layer. The Py layer is necessary to make the magnetic layer soft and a Co layer is needed to reach a high spin polarisation. The Co is at the interface between the ferromagnet and the insulator, because the TMR-effect increases with a increasing polarisation. As an insulating barrier Al (0.85 nm) is used, which has been oxidated for 8 sec. Below the junction is a IrMn layer, an antiferromagnet, which exchange bias the second ferromagnet. To grow a good antiferromagnet a Py layer is used. To get a flat Py layer, this layer is grown on a Ta layer.
Figure 4.2 shows an overview of the seven tunnel junctions. They are visible at the v-point. The big electrodes are necessary to contact the junction, because the tunnel junctions itself is to small to connect it with a wire. The junctions are microfabricated and used in the following sizes: $(10, 20, 50, 70\mu\text{m}) \times 10\mu\text{m}$ (figure 4.3).

4.2 Experiment

We want to measure the noise of a tunnel junction. Figure 4.3 shows the measurement. A current is driven through the sample. The AC voltage over the sample is measured. Because the amplifier produces extra noise and also the leads pick up noise from the surrounding, the voltage is measured twice and each signal is amplified a 100 times by an other amplifier.In this way a distinction can be made between the noise from the sample and the additional noise caused by the amplifiers and the leads. This distinction is done in a digital signal analyser, which takes the cross correlation of the two signals and averages out the signal of the junction. It calculates the cross spectrum $S_V(\omega)$ and sends it to a computer, where it can be post processed. To avoid aliasing a lowpass filter is used between the amplifiers an the signal analyser.
Two orthogonal pair of Helmholtz coils are used to apply a magnetic field at the sample position. With a power supply a current is driven through this coils. By changing this current the field can be varied. The current is adjusted by a voltage from a function generator, which produces a sinewave voltage. When the field at the sample position has the desired value, the function generator stops and the field is stable. To reduce the noise and the drift in the voltage of the function generator a lowpass filter is used. The coils are

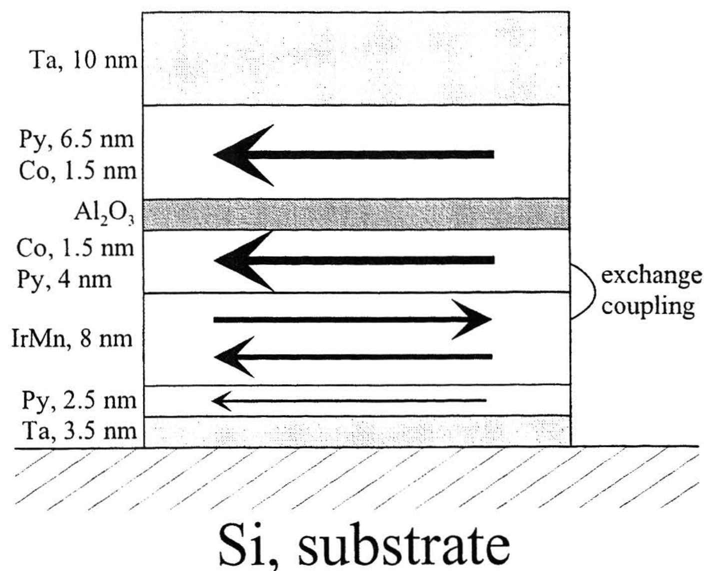

Figure 4.1: Here the structure of the tunnel junction is shown. The barrier consists of a 0.85 nm thick Al layer, which is oxidated for 8 sec.

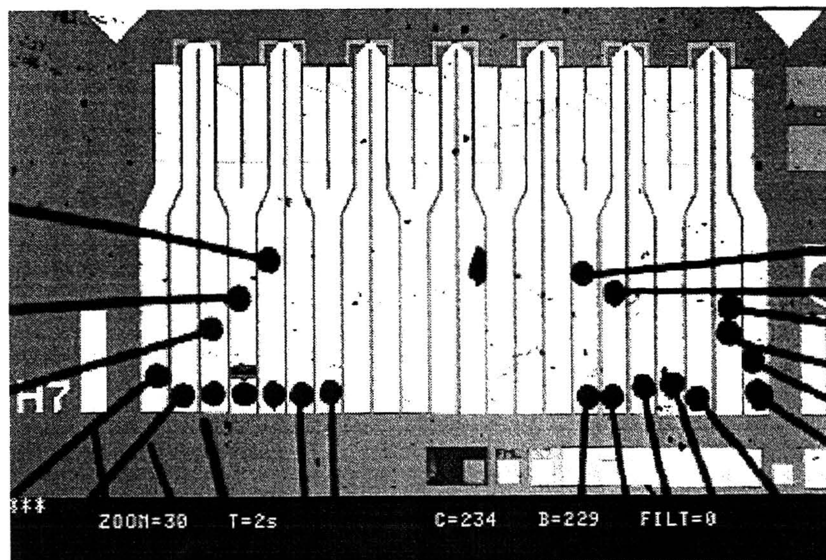

Figure 4.2: The figure shows the used samples. At the top of the V-shaped contacts are the tunnel junctions with a size of $(70, 50, 20, 20, 20, 20, 10\mu\text{m}) \times 10\mu\text{m}$; going form the left to the right. The black wires are the electrical contacts.

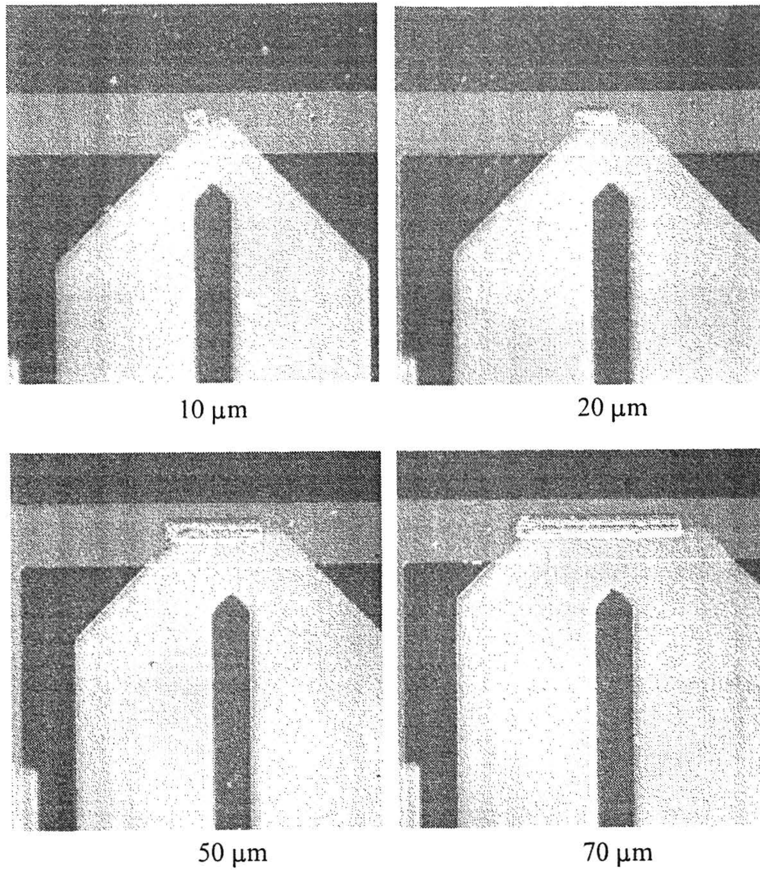

Figure 4.3: This is a close-up of the tunnel junctions. Four types of junctions are shown with a width of 10μm, 20μm, 50μm and 70μm and a height of 10μm.

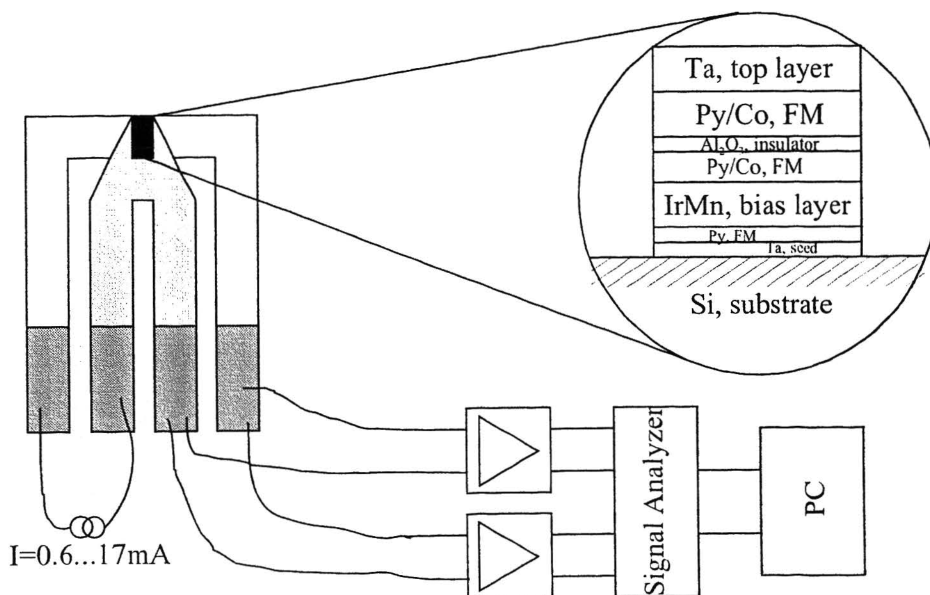

Figure 4.4: This is the schematical setup for measuring noise of the used tunnel junctions.

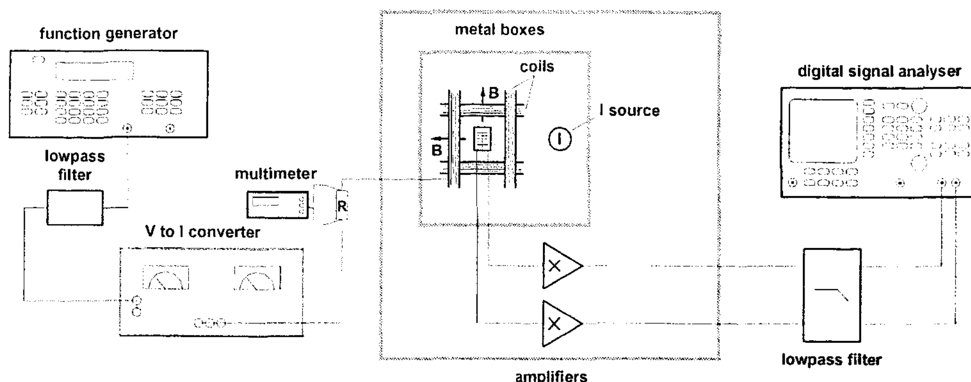

Figure 4.5: This is the setup used for all maesurements. All instruments are connected with a computer.

water cooled, therefore there is no drift in the current through the coils due to thermal heating of the coils.

To avoid any influence from the surrounding everything has to be shielded well. Due to that the junction together with the current source and the coils are placed in a μ-metal box, which itself is together with the amplifiers and the batteries in a second μ-metal box. The amplifiers and the current source are battery operated, because this reduces the 50 Hz noise from the net.

On the computer a fit program is used to extract the 1/f noise from the spectrum. It uses white noise, 1/f noise, Lorentzians and correction term for the low pass filter. The program fits the following equation to the data,

$$fit = \frac{a}{f^{\gamma}} + c, \tag{4.1}$$

where a, γ and c are fit parameters, which are stored in a file. The resulted a still depends on both the number of charged carriers N and the applied voltage V, see equation 3.17. N has no meaning for a tunnel junction. Therefore a is corrected only for the voltage,

$$\beta := \frac{a}{V(H)^2}. \tag{4.2}$$

This value can then be measured as a function of the applied field.

Chapter 5

Measurements

5.1 Resistance versus Field

The resistance of a tunnel junction as a function of the applied field is measured. Using the function generator with a low frequency < 0.1Hz the field is changed slowly and during this change a multimeter measures the voltage U over the junction. Because the current I is kept constant the changing in resistance can be calculated.
Figure 5.1 shows the resistance of a 20μm $\times$ 10μm junction for different currents I. At high negative fields the magnetisation both ferromagnets are parallel aligned and therefore the resistance is low. For zero field the parallel alignment is conserved and the free layer does not switch, because there is a ferromagnetical coupling between the two ferromagnets. To overcome this coupling a small field is necessary. Then the free layer switches and the resistance becomes higher. At high negative fields also the magnetisation of the biased (bottom) layer changes. In this case both magnetisations are again parallel aligned and the resistance becomes again low.
The resistance also depends on the current (figure 5.1), because Ohms law is not valid for a tunnel junction. While measuring changing the field very slowly small jumps are observed in the resistance (figure 5.1). The jumps are very small and seemed to be different for both different currents and junctions. Probably they are due to the switching of small domains in the layers.

5.2 Current dependence of the MR-Ratio

Out of the resistance the MR-ratio can be calculated,

$$MR = \frac{R_{AP} - R_P}{R_P}. \tag{5.1}$$

Figure 5.2 shows a plot of the MR-ratio for different currents and points out, that the ratio strongly depends on the current.

With increasing current the MR-ratio becomes lower and the plateau for the antiparallel state smaller. The field at which the top layer switches does not change, but only the position at which the bottom, strong coupled layer moves, changes. The shift is reversible and does not depend on the sign of the current. It could be due to a heating of the junction. If the current density is not homogeneous over the sample, only few points contibute the main current. This causes so called hot spots, point with a higher temperature than the rest of the sample. If the temperature increases the exchange bias field decreases and

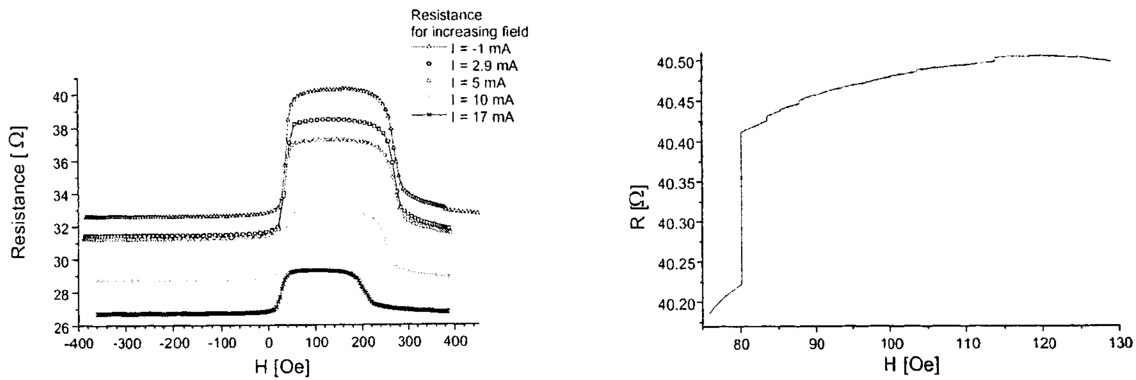

Figure 5.1: In the left graph the resistance R of the junction for different currents I is plotted over the field H. The right plot shows a detailed measurement of the resistance of the junction in the antiparallel state. One large jump and several small jumps are observed.

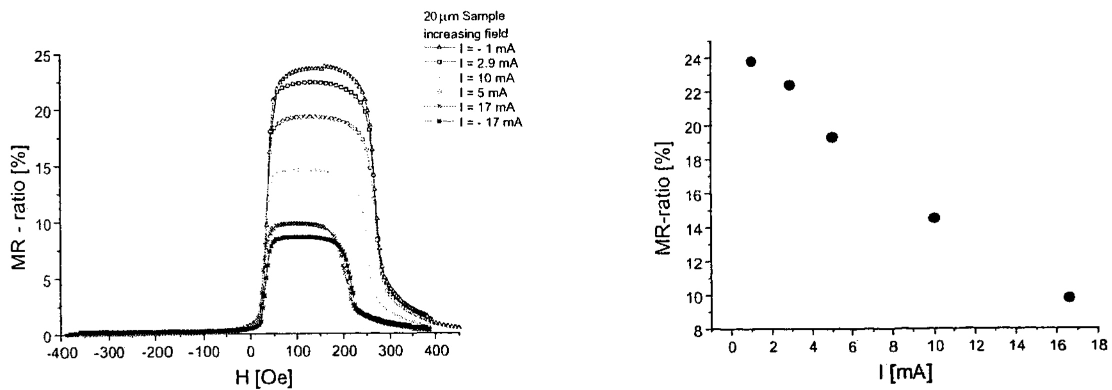

Figure 5.2: The left graph shows the MR-ratio versus the field H of a 20μm $\times$ 10μm junction for different currents I. In the right graph the dependence of the MR-ratio on the current I is plotted for the same sample. For an increasing current the ratio becomes lower.

the bias ferromagnetic layer switches earlier.
The MR-ratio depends also on the direction of the current, because for negative currents the MR-ratio is lower than for positive ones.

5.3 White Noise

The white noise level S_V depends on the applied current (equation 3.14). The junction with the highest resistance is the one with an area of $100\mu m^2$ and a resistance of about 60Ω. This resistance is low compared with a resistance of about 300Ω of the contacts. Therefore the measured white noise is maily contributed by the contacts and not by the junction. Because of this bad conditions for measuring white noise only $1/f$-noise can be observed.

5.4 $1/f$-Noise

5.4.1 $1/f$-Noise versus Field

These $\beta := \frac{\alpha}{N}$ noise measurements are done in the following way: the computer increases the field by about 2 Oe using the function generator. Then the signal analyser makes a measurement of the noise and send it to the computer. After that the procedure starts again.
The field H range for the measurements is -400 Oe to 400 Oe. With the used setup it was not possible to saturate the ferromagnet, therefore only the increasing field is measured. Figure (5.3) shows such a $1/f$-noise measurement. It starts always at high negative fields to create a good begin situation. In this part the noise is on a low level and stays there till the field is close to zero. Then the noise starts to increase and for low positive fields a peak appears. It is caused by the movement of the magnetisation of the free layer. This layer is not really free, but there is a small coupling between the two ferromagnets. To overcome this ferromagnetical coupling a field is necessary and therefore the peak is not at zero but at a little higher field. Both magnetisations are antiparallel aligned now. In this part also the 1/f noise is on a much higher level than for the parallel case. A further increase of the field results a second peak at the position, where the magnetisation direction of the bias layer changes. This peak is wider than the first one. It can be explained by the strong coupling between the antiferromagnet and the ferromagnet, which causes a slower switching. At high positive fields the noise seems to go back to its low level, but with the used setup it is not possible to reach such high fields to proof this.
It is not really clear, if the noise in the antiparallel state is really at a higher. The higher level seen in figure (5.3) can also be due to a overlapping of the two peaks. To proof this, a junction with a wider antiparallel state is necessary.

5.4.2 Current dependence of $1/f$-Noise

Now the noise is measured for different currents. Figure (5.4) shows that the noise level at negative fields is almost constant. The small increases for higher currents can be caused by a heating up of the sample. In the antiparallel state of the magnetisation the level decreases for increasing current. The peak on the left side of this plateau does not change, but the peak on the right side becomes smaller and moves to the left, because the switch-field decreases.

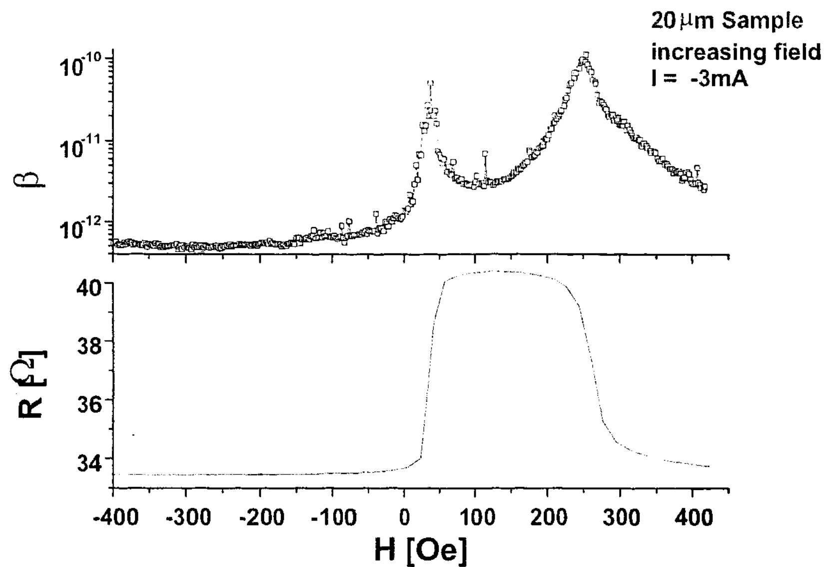

Figure 5.3: The plateau in the $1/f$-noise seems to be caused by the antiparallel alignment of the magnetisation directions in the ferromagnets.

In the antiparallel state often two spikes are visible. They should be caused by a step in the resistance, but measurements do not verify this.

The changing in noise depending on the alignment is very high. A ratio for the noise change is defined as

$$NC := \frac{\frac{S_{V,AP}}{V_{AP}^2} - \frac{S_{V,P}}{V_P^2}}{\frac{S_{V,P}}{V_P^2}} = \frac{\beta_{AP} - \beta_P}{\beta_P}, \tag{5.2}$$

where S_V are the measured values of the $1/f$-noise in the parallel (P) and antiparallel (AP) state (figure 5.5).

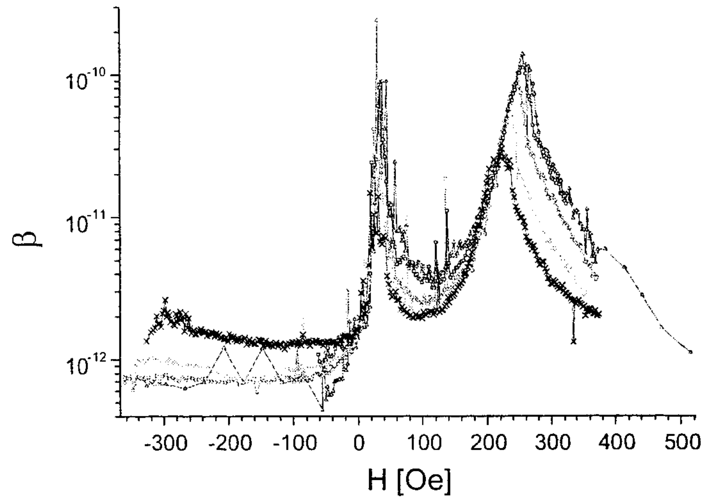

Figure 5.4: The $1/f$-noise for different currents $I = -1, 2.9, 5, 10, 16.6$ mA is plotted over the field H.

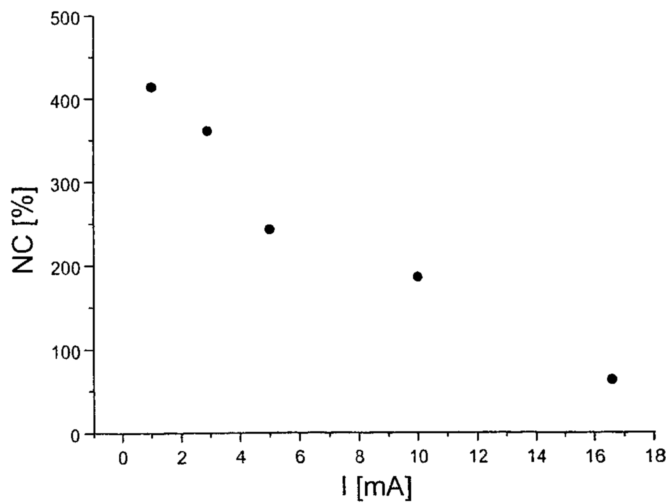

Figure 5.5: The plot shows the current dependence of the MR-ratio. For an increasing current the MR-ratio decreases.

Chapter 6

Discussions

During this work the 1/f noise and the MR-ratio in a ferromagnetic tunnel junction was observed. The results of the measurements show, that the MR-ratio decreases for an increasing current. Also the antiparallel state of the magnetisation becomes smaller, which is dued to a heating up effect of the sample.
The 1/f noise depends on the alignment of the magnetisation directions of the ferromagnets, too. In the parallel case the noise is low and in the antiparallel situation it is much higher. For different currents the low noise level does not change, while the high noise level decreases for an increasing current. On both sides of the high 1/f noise level two peaks are visible, which are the result of the switching magnetisation direction. The right peak decreases for increasing currents, becauses the switchfield changes.
An other point is, that there is never a real plateau seen in the antiparallel state. What is seen is, that the noise decreased, reached a minimum and increased again. This "plateau" can be also caused by an overlapping of the two big peaks on the left and on the right. This can be investigated using a new junction with a wider plateau in the MR-ratio.
If there are two different levels a noise ratio can be defined as

$$NC := \frac{\beta_{AP} - \beta_P}{\beta_P}, \tag{6.1}$$

where β is the spectral noise intensity corrected for the voltage and for the frequency. NC-ratios up to 450% are observed. To compare this with theoretical calculations the Julliere model can be used. In this model the parallel P and antiparallel AP conductance is given as,

$$\begin{aligned} G_P &= \frac{c}{2}(p^2 +) && (6.2) \\ G_{AP} &= \frac{c}{2}(1 - P^2), && (6.3) \end{aligned}$$

where c is just a constant and p means the polarisation. If there are fluctuations in the polarisation, this results fluctuations in conductivity. The spectral density of the conductivity fluctuations S_G is,

$$S_G = \left(\frac{\partial G}{\partial P}\right)^2 S_P, \tag{6.4}$$

where S_P is the spectral density of polarisation fluctuations. Applying this equation on (6.2) and (6.3), S_G is the same in both the antiparalel and parallel state,

$$S_{G,P} = S_{G,AP}. \tag{6.5}$$

Using the following general equation,

$$S_V = \left(\frac{\partial V}{\partial G}\right)^2 S_G, \tag{6.6}$$

the spectral noise density S_V becomes

$$\frac{S_V}{V^2} = \frac{S_G}{G^2}. \tag{6.7}$$

Using this for a MR-ratio of 19% the calculated change in $1/f$-noise becomes 42%. Compared with the measured value of about 250% this could not be right.
As already noticed before (see chapter about MR-ratio)one feature of the Julliere model is the independence of the MR-ratio on the barrier geometry. The calculation says that the ratio of the noise levels does neither depend on fluctuations in the thickness nor on fluctuations in the height.
Using a free electron model [13] it is possible to calculate such high change for the NC-ratio. S_E is the noise due to changes in the conductance band. If the bottom of the band fluctuates it results noise in the current,

$$S_I = \left(\frac{\partial I}{\partial E}\right)^2 S_E. \tag{6.8}$$

The result of these calculations is shown in figure (6.1). The comparing with figure (5.5) shows, that the trend is the same. For a tunnel junction with a MR-ratio of 38% a NC-ratio of about 900% can be get.
In the resistance versus field curve small jumps are seen. It could be, that these are switching domains, but no coherence between these jumps and the 1/f noise can be seen. A reasonable explanation could be, that it is not possible to measure it with the this setup. A average over the time is used, therefore the resulted peak of such a moving domain would be averaged out or results an overload in the signal analyser. Although it would be exspectable, which describes a correlation between the

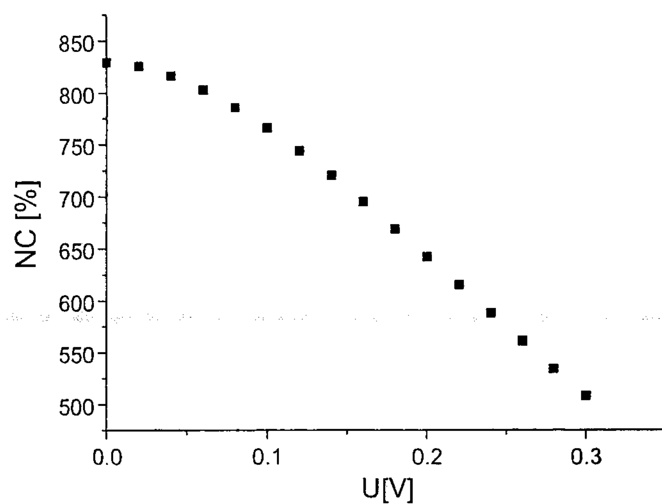

Figure 6.1: The figure shows a plot of the theoretical calculations using a free electron model.

Acknowledgement

From december 1999 to march 2000 I did a traineeship at the TUE in the group "Physic of Nanostructures". First of all I want to thank my supervisor Bart Smits for all his help, explanations, discussions, advices and for correcting this report. I guess, it was not that easy with me.
Thanks to Philips for making the junctions and especially to Reinder Coehoorn for the discussions and the theoretical calculations. Further on I thank Maarten van Kampen and Corné Kant for some figures I could use in my report, especially to Corné, who had to share the lab with me, and Jef Noijen for the technical support.

Bibliography

[1] T. R. McGuire and R. I. Potter, IEEE Trans. Magn. **11**, 1018 (1975).

[2] P. Grünberg, G. Binasch, F. Saurenbach, and W. Zinn, Phys. Rev. B **39**, 4828 (1989).

[3] M. Julliere, Phys. Lett. **54A**, 225 (1975).

[4] J. S. Moodera, L. R. Kinder, T. M. Wong, and R. Meservey, Phys. Rev. Lett. **74**, 3273 (1995).

[5] C. H. Kant, Master's thesis, Technische Universiteit Eindhoven, 1998.

[6] J. C. Slonczewski, Phys. Rev. B **39**, 6995 (1989).

[7] S. Kogan, *Electronic noise and fluctuations in solids* (Cambridge University Press, Cambridge, 1996).

[8] M. J. Buckingham, Noise in electronic devices and systems, Ellis Horwood Limited (1983).

[9] M. van Kampen, Master's thesis, Technische Universiteit Eindhoven, 1998.

[10] G. Lecoy and L. Gouskov, Phys. Status Solidi **39**, 9 (1968).

[11] F. N. Hooge, Physica **83B**, 14 (1976).

[12] R. van de Veerdonk *et al.*, J. Appl. Phys. **82**, 6152 (1997).

[13] J. M. MacLaren, X. G. Zhang, and W. H. Butler, Phys. Rev. B **56**, 827 (1997).

[14] H. Vogel, *Gerthsen Physik* (Springer- Verlag Berlin Heidelberg, Berlin, 1997).

[15] I. N. Bronstein and K. A. Semendjajew, *Teubner- Taschenbuch der Mathematik Teil 1* (B. G. Teubner Verlagsgesellschaft Leipzig, Leipzig, 1996).

[16] *Taschenbuch der Physik*, 3 ed., edited by H. Stoecker (Verlag Harri Deutsch, Berlin, 1998).

[17] diverse, in *Teubner- Taschenbuch der Mathematik Teil 2*, edited by G. Grosche, E. Zeidler, D. Ziegler, and V. Ziegler (B. G. Teubner Verlagsgesellschaft Leipzig, Leipzig, 1995).